Proceedings of the INMM & ESARDA Joint Virtual Annual Meeting
August 23-26 & August 30-September 1, 2021

PASSIVE NEUTRON ALBEDO REACTIVITY MEASUREMENTS OF SPENT BWR FUEL

T. Tupasela[1], T. Honkamaa[1], M. Moring[1], P. Dendooven[2]

[1] STUK – Radiation and Nuclear Safety Authority, Finland
[2] Helsinki Institute of Physics, University of Helsinki, Finland

ABSTRACT

Before geological disposal of spent nuclear fuel in Finland, the integrity of each fuel assembly will be verified. Passive Neutron Albedo Reactivity (PNAR) verification is part of the national non-destructive verification concept, developed by the Finnish Radiation and Nuclear Safety Authority (STUK). PNAR verification utilizes the neutron radiation of the spent fuel itself to measure neutron multiplication in the assembly. Thus, it can be used to verify the presence of fissile material. A PNAR instrument was built and tested for the first time in 2019 in a collaboration led by STUK. In 2020, a second measurement campaign was held at the Olkiluoto spent fuel storage. Several BWR-type assemblies of different designs and operational histories were measured to understand the PNAR's response to different fuel parameters. Axial measurements of the same assembly reveal an axial multiplication profile in the fuel. From the multiplication profiles, the decrease of fissile content caused by partial length rods can be identified. The uncertainty of a PNAR measurement was studied with repeated measurements. The results show that a typical PNAR measurement, with a total measurement time of six minutes, has a dynamic range of approximately 70 standard deviations. Based on the measurements performed in 2019 and 2020, PNAR can quantify the neutron multiplication of a spent fuel assembly with great precision and assemblies of different histories can be discerned from each other. The multiplication measurement result can be used to verify the assembly declaration and to detect partial defects. The PNAR method is constantly being developed. Our aim is to have the method ready for application in 2025.

INTRODUCTION

Disposal of spent nuclear fuel into a geological repository is expected to begin in Finland in 2025. Geological disposal is a unique challenge to nuclear safeguards, as verification of the fuel items becomes extremely difficult after the fuel is encapsulated to Finnish bedrock. Therefore, fuel assembly verification prior to encapsulation is an important task. The Finnish concept for nuclear safeguards of geological repositories [1], developed by STUK – the Finnish Radiation and Nuclear Safety Authority, includes verification of the declaration of each fuel item, using the best available technology. Currently, the chosen technology is a combined measurement using two different NDA (non-destructive assay) instruments – PGET (Passive Gamma Emission Tomography) and PNAR (Passive Neutron Albedo Reactivity). PGET takes a tomographic gamma image of a fuel assembly, from which the presence of single fuel pins can be verified [2-4]. PGET was approved as a verification instrument in 2017 by the IAEA (International Atomic Energy Agency). PNAR measures neutron multiplication and therefore verifies the presence of fissile material [5-7]. STUK, in collaboration with Encapsulation NDA Services, the Helsinki Institute of Physics and Provedos Oy, simulated [8-10], designed and built a prototype PNAR instrument to study the

capabilities of PNAR NDA [6,7]. The prototype is designed especially for the BWR type fuel used in the Olkiluoto nuclear power plant (NPP). The very first fuel measurements were performed in 2019 [11]. Two subsequent measurement campaigns were successfully performed in the fall of 2020 and summer of 2021. This paper introduces new results and findings based on the data gathered in the measurement campaigns.

The operating principle of a PNAR detector as well as the design of the STUK PNAR prototype has been introduced in detail in other work [6-8]. Thus, only a brief summary is given in this article. Spent nuclear fuel in Finland is stored in wet interim storages. The PNAR measurement is performed in the fuel storage pool. PNAR utilizes the albedo of the neutron radiation of the spent fuel to assay the neutron multiplication of a fuel assembly. In practice, this is achieved by making two separate measurements – one with a cadmium liner between the fuel and the PNAR's neutron detectors and one without the liner. With the cadmium liner present, the thermal neutron flux in the moderator region just outside the fuel assembly is suppressed, effectively reducing the neutron albedo.

STUK's PNAR instrument is composed of four identical detector pods arranged into a square with a central opening. The fuel assembly to be measured and the movable cadmium liner are located in the central opening. The PNAR instrument is designed to be a tight fit around the BWR fuel used in Olkiluoto NPP. Having the cadmium liner close to the fuel assembly is crucial for measurement sensitivity. Each detector pod holds one He-3 proportional neutron detector and one ionization chamber for gross gamma detection. The neutron detectors are embedded in polyethylene and completely lined with cadmium to make the neutron measurement sensitive to fast neutrons. Figure 1 shows a cross sectional illustration of the design of the STUK's PNAR instrument and a picture of a fuel assembly being lowered into the PNAR's measurement position.

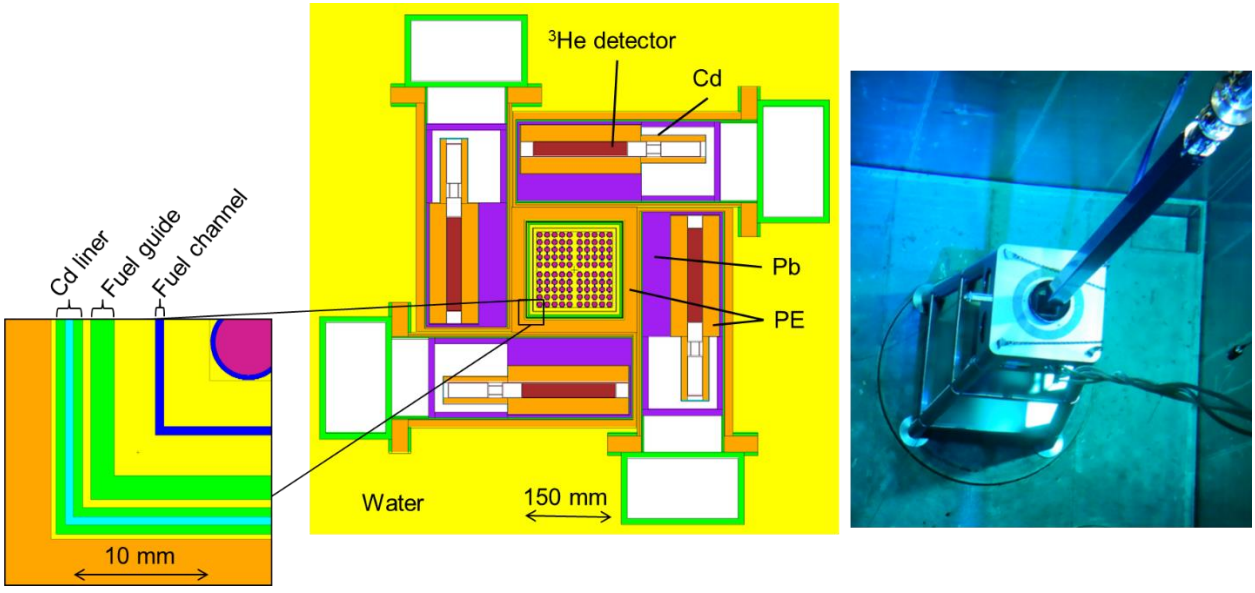

Figure 1: Left: Cross sectional image of the PNAR instrument. The measured fuel assembly is located in the middle of four identical detector pods. The movable cadmium liner is positioned very close to the fuel assembly. Right: A fuel assembly being lowered into the PNAR instrument in its support structure. (Picture: TVO)

Table 1: The basic characteristics of all measured assemblies and the respective measurement years.

ID	Assembly type	IE (%)	Burnup (MWd/tU)	Year of discharge	2019	2020	2021
1	8x8-1	1.9	18600	1984	x		x
2	8x8-1	2.9	31200	1990	x		
3	SVEA-64	3.0	34000	1998	x		
4	SVEA-64	3.0	37600	1998	x	x	x
5	SVEA-64	3.0	19800	1996	x		
6	SVEA-64	3.0	33000	1999	x		
11	SVEA-64	3.0	32900	1998	x		
13	SVEA-64	3.0	35700	1998	x		
16	9x9-1AB	3.2	29200	1994		x	
18	9x9-1AB	3.2	35400	1996	x		
20	ATRIUM10	3.2	37100	2002	x		
22	SVEA-100	3.2	37600	2000	x		
23	SVEA-64	3.0	33900	1998	x		
24	SVEA-64	3.0	33200	1998	x	x	
28	SVEA-64	3.0	32600	1998	x	x	x
29	SVEA-64	3.0	35700	1998		x	
30	9x9-1AB	3.2	35000	1998	x		
31	9x9-1AB	3.2	35900	1998	x		
32	9x9-1AB	3.2	35900	1998			x
35	SVEA-96 Optima	3.2	39800	2005	x		
39	ATRIUM10	3.2	35000	2002	x		
40	ATRIUM10	3.2	43200	2006		x	
42	GE12	3.2	36300	2002	x		
43	GE12	3.2	43100	2007	x		x
44	GE14	3.5	42200	2009	x		
46	GE14	3.5	43300	2013	x		x
48	ATRIUM10	3.6	49700	2008			x
49	ATRIUM10	3.6	49700	2008	x		x
51	SVEA-64	3.0	32600	1998		x	
52	ATRIUM10	3.2	36600	2006		x	x
53	SVEA-64	3.0	34100	1998		x	
54	SVEA-96 Optima	3.2	36200	2005		x	
55	GE12	3.2	41300	2003		x	
56	GE12	3.2	38600	2004		x	
57	9x9-1AB	3.2	35400	1998			x
58	SVEA-64	3.0	37300	1998			x
59	SVEA-100	3.0	33200	1999			x
60	ATRIUM10	3.2	43200	2006			x
61	ATRIUM10	3.2	44300	2008			x
62	SVEA-96 Optima	3.2	35400	2005			x
63	SVEA-96 Optima	3.2	43000	2007			x
64	SVEA-96 Optima	3.5	39800	2009			x
65	SVEA-96 Optima	3.5	40200	2010			x
66	GE12	3.2	34900	2003			x
67	GE12	3.2	35300	2004			x
68	GE12	3.2	40800	2004			x
69	GE14	3.5	47400	2012			x

MEASUREMENT CAMPAIGNS

In 2019-2021, a total of 47 different BWR fuel assemblies were measured. The initial enrichments (IE) range from 1.9 % to 3.6 %, burnup (BU) from 18600 to 49700 MWd/tU and cooling times (CT) from 6 to 37 years. All measured assemblies, together with their designs, basic operational characteristics and the years in which they were measured are listed in Table 1. All of the assemblies were measured from a default measurement height, where the neutron detectors are centred approximately one meter above the lower end of the active fuel part. Additionally, some of the assemblies were measured at multiple axial locations to quantify the axial profile of the PNAR Ratio. One assembly (#4) was measured a total of six times in 2019-2020 to quantify measurement repeatability/uncertainty.

In the 2019 measurement campaign, because of a water leak in one of the detector pods, and the usefulness of preserving symmetry, only the two operational opposite detector pods were utilized. In 2020 and 2021 all measurement pods were available. With similar measurement time of approximately 6 minutes per assembly in all campaigns, this means that twice as many counts were detected in the two later campaigns. A typical measurement consists of 2 minutes of measuring time with the cadmium liner in place and 2 minutes without the cadmium liner. Another 2 minutes are allocated to moving of the cadmium liner and saving the data.

RESULTS

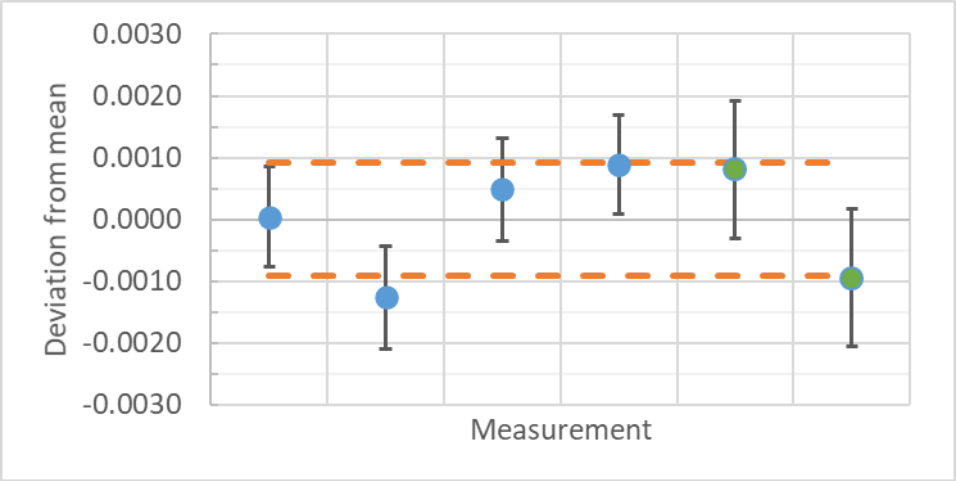

Figure 2: Deviation from the mean PNAR Ratio for the repeated measurements on assembly #4. Measurements from 2019 in green (last 2, with bigger error bars). Dashed lines indicate +/- one sample standard deviations. Error bars indicate the ±1 standard deviation counting statistical errors of each measurement.

Repeated measurements

Assembly #4 (38 GWd BU, 21/22 years CT) was measured 4 separate times in 2020. After each measurement it was returned to its original storage position and other assemblies were measured before the next repetition. Also in 2019, the same assembly was measured twice in a similar manner. The one-year difference in cooling time has no detectable influence on the PNAR Ratio. Thus, all 6 data points can be used to estimate single measurement uncertainty. However, it should be kept in mind that in 2019 only 2 pods were used to calculate the PNAR Ratio. The mean PNAR Ratio of the six measurements is 1.0438 and the sample standard deviation is 0.0009 or 0.09%. For comparison, the single measurement uncertainty, from counting statistics, in the 2020

measurements was typically 0.0007. Figure 2 shows the deviation from the mean for each single measurement together with counting statistical uncertainties.

PNAR Ratios at default measurement height

Figure 3 presents the PNAR Ratios at the default measurement height for all measured fuel assemblies to date against assembly burnups, grouped based on the assembly initial enrichment. The one standard deviation error bars calculated from counting statistics are hidden by the markers. The bottom of the vertical axis is set to 0.97, which is the simulated response of a non-multiplying fuel assembly [11]. The gap between the data points and the axis bottom is the dynamic range of the measurement. Comparing the size of this gap to the single measurement uncertainty shows that the dynamic range of a typical PNAR Ratio measurement is approximately 70 standard deviations.

It is the will of an operator to fully utilize the reactivity of each fuel assembly, i.e. maximize the burnup for given initial enrichment, within their given safety limits. As seen in Figure 3, fully burnt assemblies, with burnup generally increasing with IE, have a PNAR Ratio within the range of 1.03-1.05. When an assembly is not fully burnt, i.e. it has more fissile material remaining than a similar fully burnt assembly, its PNAR Ratio is higher and such an assembly will be located in the top left part of Figure 3.

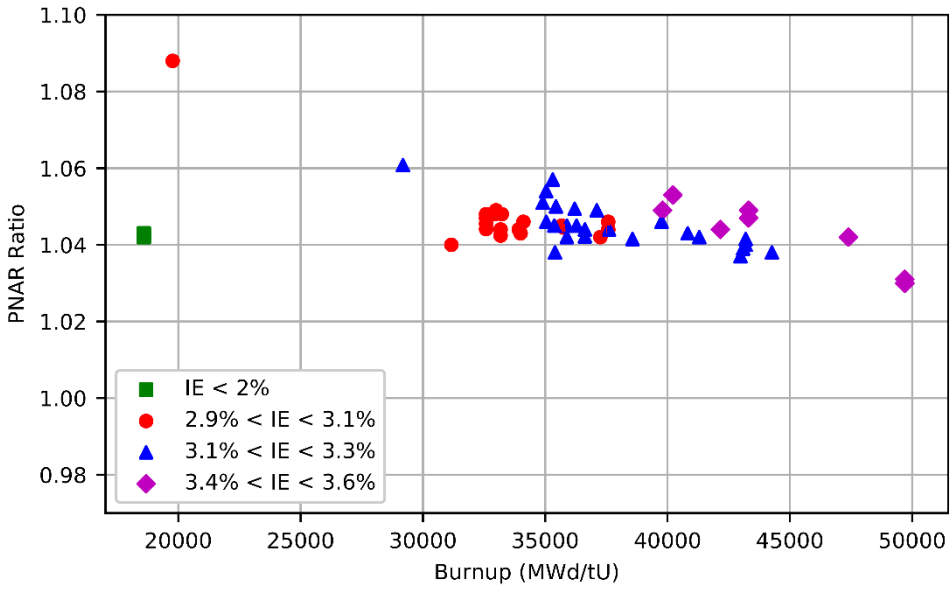

Figure 3: PNAR Ratios at the default measurement height compared to assembly burnup of all fuel assemblies measured in 2019-2021 combined. The assemblies are grouped based on their initial enrichment (IE). The bottom of the vertical axis (0.97) is the simulated response of a non-multiplying assembly.

Axial PNAR Ratio profile

In 2020, several assemblies were measured at multiple axial levels. Figure 4 shows the PNAR Ratios at the different measurement heights for the 6 assemblies that were measured at least from 3 different heights. Generally, we see an increasing trend in the PNAR Ratios towards the top of the assemblies, meaning that the assemblies have more fissile material remaining in the top end

than in the bottom end. This observation is in line with the uneven burnup distribution of BWR assemblies and is linked to the void fraction profile in an operating BWR core.

Based on its initial enrichment and burnup, assembly #16 is less irradiated than the other assemblies. This is also seen from the PNAR Ratio, which is higher at all measurement heights compared to the other assemblies.

Assembly #4 was axially scanned both in 2020 and in 2019 and the results from 2019 are also shown in Figure 4. One year of cooling did not affect the response: the measurement results are within each other's statistical uncertainty.

Most notably for assembly #55, the PNAR Ratio decreases drastically towards the highest measurement location. This is caused by the ending of partial length rods at approximately 2600 mm from the bottom of the assembly.

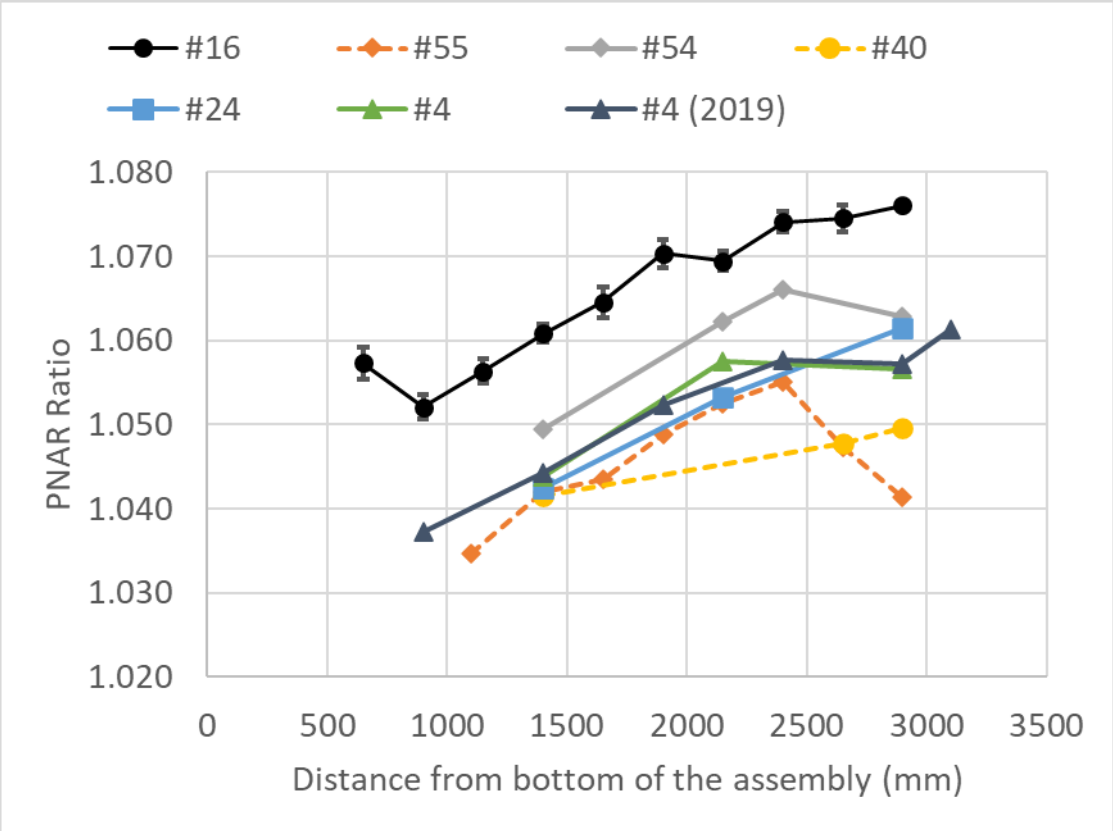

Figure 4: Axial PNAR variation on all assemblies that were measured at 3 heights or more in the 2020 measurement campaign. The axial scan results for assembly #4 from 2019 is also shown. Shorter measurement times were used on #16 resulting in larger uncertainties. For the other assemblies, error bars are smaller than the size of the markers and were hidden. The default measurement height is at 1400 mm.

Simulating missing pins with partial length rods

Several fuel assemblies were measured from heights of 2400 mm and 2900 mm, relative to the scale in Figure 4. These measurement points are located on both sides of the axial location where

2/3-length partial fuel rods end. The older BWR fuel types in Olkiluoto have no partial length rods, while the newer types include several different partial length rod layouts. The absence of the partial length rods in the higher measurement positions can be used to simulate missing fuel pins. Figure 5 shows the pin layout of SVEA-96 Optima (assembly #54) and GE12 (assembly #55) fuel assemblies at these two heights. Optima has 8 partial length rods while GE12 has 14. The locations of the partial length rods, and the water channels, are also different.

Table 2 compares the measured PNAR Ratios of assemblies #4 (SVEA-64, no partial length rods), #54 (SVEA-96 Optima) and #55 (GE12), the latter 2 designs presented in Figure 5, at the two measurement heights, 2400 mm and 2900 mm. MCNP6.2 simulated PNAR Ratios of the two cases are also presented. The simulation is based on a representative fuel assembly with 3 % IE, 30 GWd/tU BU and 20 a CT with a homogeneous fuel mixture between all fuel rods. The only difference between the simulations was the pin layouts as presented in Figure 5.

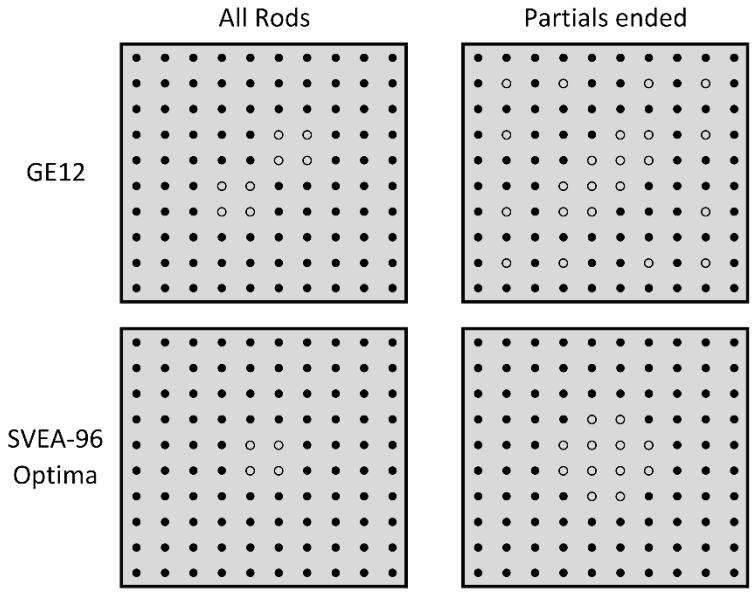

Figure 5: The pin layout in GE12 and SVEA-96 Optima assemblies with and without the partial length rods. The empty positions in the All Rods column are water channels.

Table 2: Measured and simulated PNAR Ratios before and after the ending of partial length rods of GE12 and SVEA-96 Optima assemblies and measured PNAR Ratios of a SVEA-64 assembly with no partial length rods.

	Measurements			**Simulations**	
	Svea-64	**GE12**	**Optima**	**GE12**	**Optima**
2900 mm	1.057 ±0.001	1.0414 ±0.0005	1.0629 ±0.0009	1.078 ±0.004	1.085 ±0.004
2400 mm	1.058 ±0.001	1.055 ±0.0005	1.0661 ±0.0007	1.087 ±0.004	1.089 ±0.004
Change in material	0%	-13%	-8.4%	-13%	-8.4%
Change in PNAR Ratio	0%	-1.29% ±0.08%	-0.30% ±0.11%	-0.83%	-0.37%

The measurement results in Table 2 show that the PNAR Ratio decreases significantly over the two measurement positions, when compared to the uncertainty of an individual measurement, in both assemblies with partial length rods. For the control assembly without partial length rods, the PNAR Ratio stays the same. The PNAR Ratio decrease is larger for the GE12 assembly which also has more partial length rods. However, the change in PNAR Ratios are not directly proportional to the change of fuel material present. The locations of the missing fuel rods also affect the PNAR Ratio. The PNAR utilizes passive albedo neutrons to assay assembly multiplication and is therefore more sensitive to the outermost rods of a fuel assembly. Still, we see from the measurements of the SVEA-96 Optima assembly that the innermost rods are not completely shielded by the rest of the fuel.

The simulation results seem to underestimate the change in PNAR Ratio for the GE12 assembly. The difference between the simulated and measurements is likely caused by the simplified fuel isotopic composition used in the MCNP model.

As the two measurements are taken from different heights, the measurements are not exactly the same case as if fuel rods were removed between the two measurements. As is seen from Figure 4, the axial PNAR Ratio usually has an increasing trend towards the top of an assembly. However, the axial measurements also indicate that the axial PNAR Ratio profile flattens near the top of the assembly. For the of a SVEA-64 assembly (#4) without partial length rods, PNAR Ratio does not significantly change over the two measurement locations of 2400 mm and 2900 mm.

CONCLUSIONS

47 different BWR spent fuel assemblies were measured with STUK's PNAR instrument in 2019-2021. Fully burnt fuel assemblies consistently measure a PNAR Ratio between 1.03 and 1.05, while the PNAR Ratio is larger for assemblies with more remaining fissile material. Repeated measurements of a single assembly indicate a measurement uncertainty of 0.009, resulting into a dynamic range of approximately 70 standard deviations for the PNAR measurement. The repeated measurements were taken in 2 different campaigns that had 1 year between them. Still, the PNAR Ratios measured were the same.

Axial PNAR Ratio profiles were also measured for different type of assemblies. Typically, the PNAR Ratio increases towards the top of an assembly and flattens or starts to decrease near the top of the assembly. For assemblies with partial length rods, the decrease of PNAR Ratio near the top of the assemblies was larger. For one assembly that was clearly not fully irradiated, based on its IE and BU, the PNAR Ratio was elevated at all axial positions when compared to other fully irradiated assemblies.

The PNAR Ratios at locations around the level where partial length rods end were compared for three different assembly types that have 0, 8 and 14 partial length rods. The decrease of PNAR Ratio is progressively larger for the assemblies with more partial length rods. However, the change in PNAR Ratio is not only dependent on the amount of fuel material not present. Instead, the locations where the pins are removed from affect the PNAR Ratio as well. This is because PNAR utilizes passive albedo neutrons to assay assembly multiplication and is therefore more sensitive to the outermost pins of a fuel assembly. In conclusion, these measurements indicate that partial defects could be detected with PNAR. Such analysis would require the measured PNAR Ratio to be compared to a computational model that can accurately predict the expected PNAR Ratio. Annual measurement campaigns are foreseen to gather data needed for continuous development of PNAR analysis methods.

REFERENCES

[1] T. Honkamaa, M. Hämäläinen, E. Martikka, M. Moring, O. Okko, T. Tupasela, National Safeguards
Concept for Encapsulation Plant and Geological Repository, in: ESARDA 41st Annu. Meet. Symp. Safeguards Nucl. Mater. Manag. 14-16 May 2019 Stresa Italy, ESARDA, Luxembourg, 2019: pp. 235–239. https://doi.org/doi:10.2760/159550.

[2] T. White, T. Honkamaa, M. Mayorov, P. Peura, J. Dahlberg, J. Keubler, V. Ivanov, A. Turunen, Application of Passive Gamma Emission Tomography (PGET) for the Verification of Spent Nuclear Fuel, in: Proc. Inst. Nucl. Mater. Manag. Annu. Meet., Baltimore, MD, USA, 2018.

[3] C. Bélanger-Champagne, P. Peura, P. Eerola, T. Honkamaa, T. White, M. Mayorov, P. Dendooven, Effect of gamma-ray energy on image quality in Passive Gamma Emission Tomography of spent nuclear fuel. IEEE Trans. Nucl. Sci. 66 (2019) 487.

[4] R. Virta, R. Backholm, T.A. Bubba, T. Helin, M. Moring, S. Siltanen, P. Dendooven, T. Honkamaa, Fuel rod classification from Passive Gamma Emission Tomography (PGET) of spent nuclear fuel assemblies. ESARDA Bulletin 61 (2020) 10.

[5] H.O. Menlove, and D.H. Beddingfield, Passive neutron reactivity measurement technique. In Proceedings of the Institute of Nuclear Materials Management Annual Meeting (1997).

[6] S.J. Tobin, P. Peura, T. Honkamaa, P. Dendooven, M. Moring, C. Bélanger-Champagne, Passive Neutron Albedo Reactivity in the Finnish encapsulation context, 2018. http://urn.fi/URN:ISBN:978-952-309-406-2.

[7] T. Tupasela, Passive neutron albedo reactivity assay of spent nuclear fuel, G2 Pro gradu, 2019. http://urn.fi/URN:NBN:fi:aalto-201908254886.

[8] S.J. Tobin, P. Peura, C. Bélanger-Champagne, M. Moring, P. Dendooven, T. Honkamaa, Utility of including Passive Neutron Albedo Reactivity in an integrated NDA system for encapsulation safeguards. ESARDA Bulletin 56 (2018) 12.

[9] S.J. Tobin, P. Peura, C. Bélanger-Champagne, M. Moring, P. Dendooven, T. Honkamaa, Measuring spent fuel assembly multiplication in borated water with a passive neutron albedo reactivity instrument. Nucl. Instrum. Meth. Phys. Res. A 897 (2018) 32.

[10] V. Litichevskyi, P. Peura, P. Dendooven, T. Tupasela, T. Honkamaa, M. Moring, and S.J. Tobin, Effect of water gap and fuel assembly positioning in Passive Neutron Albedo Reactivity measurements for spent fuel encapsulation safeguards. J. Nucl. Materials Management 48 (2020) 22.

[11] T. Tupasela, P. Dendooven, S. J. Tobin, V. Litichevskyi, P. Koponen, A. Turunen, M. Moring, T. Honkamaa. Passive neutron albedo reactivity measurements of spent nuclear fuel. Nucl. Instrum. Meth. Phys. Res. A 986 (2021) 164707. https://doi.org/10.1016/j.nima.2020.164707